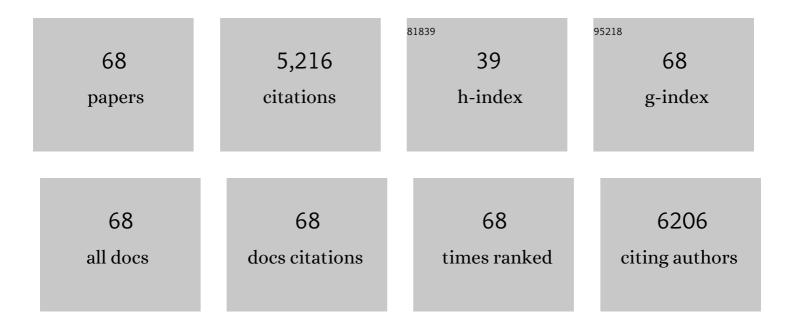
List of Publications by Year in descending order

Source: https://exaly.com/author-pdf/9159786/publications.pdf Version: 2024-02-01



#	Article	IF	CITATIONS
1	Adsorption and removal of tetracycline antibiotics from aqueous solution by graphene oxide. Journal of Colloid and Interface Science, 2012, 368, 540-546.	5.0	1,180
2	Humidity-Sensing Properties of Urchinlike CuO Nanostructures Modified by Reduced Graphene Oxide. ACS Applied Materials & Interfaces, 2014, 6, 3888-3895.	4.0	184
3	Acetone gas sensor based on NiO/ZnO hollow spheres: Fast response and recovery, and low (ppb) detection limit. Journal of Colloid and Interface Science, 2017, 495, 207-215.	5.0	182
4	NH3 gas sensing performance enhanced by Pt-loaded on mesoporous WO3. Sensors and Actuators B: Chemical, 2017, 238, 473-481.	4.0	181
5	Dual functional N- and S-co-doped carbon dots as the sensor for temperature and Fe3+ ions. Sensors and Actuators B: Chemical, 2017, 242, 1272-1280.	4.0	177
6	Room temperature NO 2 gas sensor based on porous Co 3 O 4 slices/reduced graphene oxide hybrid. Sensors and Actuators B: Chemical, 2018, 263, 387-399.	4.0	159
7	The room temperature gas sensor based on Polyaniline@flower-like WO3 nanocomposites and flexible PET substrate for NH3 detection. Sensors and Actuators B: Chemical, 2018, 259, 505-513.	4.0	159
8	Preparation of Ag-loaded mesoporous WO3 and its enhanced NO2 sensing performance. Sensors and Actuators B: Chemical, 2016, 225, 544-552.	4.0	127
9	Enhanced gas sensing properties to acetone vapor achieved by α-Fe2O3 particles ameliorated with reduced graphene oxide sheets. Sensors and Actuators B: Chemical, 2017, 241, 904-914.	4.0	124
10	Flower-like In2O3 modified by reduced graphene oxide sheets serving as a highly sensitive gas sensor for trace NO2 detection. Journal of Colloid and Interface Science, 2017, 504, 206-213.	5.0	113
11	Ultrasensitive and low detection limit of nitrogen dioxide gas sensor based on flower-like ZnO hierarchical nanostructure modified by reduced graphene oxide. Sensors and Actuators B: Chemical, 2017, 249, 715-724.	4.0	107
12	Improvement of NO2 gas sensing performance based on discoid tin oxide modified by reduced graphene oxide. Sensors and Actuators B: Chemical, 2016, 227, 419-426.	4.0	102
13	Enhanced sensitive and selective xylene sensors using W-doped NiO nanotubes. Sensors and Actuators B: Chemical, 2015, 221, 1475-1482.	4.0	101
14	Au-loaded mesoporous WO3: Preparation and n-butanol sensing performances. Sensors and Actuators B: Chemical, 2016, 236, 67-76.	4.0	92
15	Ultra-sensitive sensing platform based on Pt-ZnO-In2O3 nanofibers for detection of acetone. Sensors and Actuators B: Chemical, 2018, 272, 185-194.	4.0	90
16	A fluorescent biosensor based on molybdenum disulfide nanosheets and protein aptamer for sensitive detection of carcinoembryonic antigen. Sensors and Actuators B: Chemical, 2018, 273, 185-190.	4.0	88
17	The preparation of reduced graphene oxide-encapsulated α-Fe2O3 hybrid and its outstanding NO2 gas sensing properties at room temperature. Sensors and Actuators B: Chemical, 2018, 261, 252-263.	4.0	87
18	Flower-like WO3 architectures synthesized via a microwave-assisted method and their gas sensing properties. Sensors and Actuators B: Chemical, 2013, 186, 734-740.	4.0	76

#	Article	IF	CITATIONS
19	Horseshoe-shaped SnO2 with annulus-like mesoporous for ethanol gas sensing application. Sensors and Actuators B: Chemical, 2017, 240, 1321-1329.	4.0	76
20	Room temperature gas sensor based on tin dioxide@ polyaniline nanocomposite assembled on flexible substrate: ppb-level detection of NH3. Sensors and Actuators B: Chemical, 2019, 299, 126970.	4.0	75
21	The facile synthesis of MoO ₃ microsheets and their excellent gas-sensing performance toward triethylamine: high selectivity, excellent stability and superior repeatability. New Journal of Chemistry, 2018, 42, 15111-15120.	1.4	73
22	Highly sensitive sensors based on quasi-2D rGO/SnS2 hybrid for rapid detection of NO2 gas. Sensors and Actuators B: Chemical, 2019, 291, 216-225.	4.0	73
23	UV-activated ultrasensitive and fast reversible ppb NO2 sensing based on ZnO nanorod modified by constructing interfacial electric field with In2O3 nanoparticles. Sensors and Actuators B: Chemical, 2020, 305, 127498.	4.0	70
24	Enhanced NO2 gas sensing properties by Ag-doped hollow urchin-like In2O3 hierarchical nanostructures. Sensors and Actuators B: Chemical, 2017, 252, 418-427.	4.0	65
25	Fluorometric method for the determination of hydrogen peroxide and glucose with Fe3O4 as catalyst. Talanta, 2011, 85, 1075-1080.	2.9	62
26	Enhanced sensing response towards NO2 based on ordered mesoporous Zr-doped In2O3 with low operating temperature. Sensors and Actuators B: Chemical, 2017, 241, 806-813.	4.0	62
27	Hydrothermal synthesis and gas-sensing properties of flower-like Sn3O4. Sensors and Actuators B: Chemical, 2016, 224, 128-133.	4.0	60
28	Lower coordination Co3O4 mesoporous hierarchical microspheres for comprehensive sensitization of triethylamine vapor sensor. Journal of Hazardous Materials, 2022, 430, 128469.	6.5	59
29	Graphene oxide-based magnetic fluorescent hybrids for drug delivery and cellular imaging. Colloids and Surfaces B: Biointerfaces, 2013, 112, 128-133.	2.5	55
30	Carbon dots decorated hierarchical litchi-like In2O3 nanospheres for highly sensitive and selective NO2 detection. Sensors and Actuators B: Chemical, 2020, 304, 127272.	4.0	54
31	Protein–Inorganic Hybrid Nanoflower-Rooted Agarose Hydrogel Platform for Point-of-Care Detection of Acetylcholine. ACS Applied Materials & Interfaces, 2019, 11, 11857-11864.	4.0	53
32	The DNA controllable peroxidase mimetic activity of MoS ₂ nanosheets for constructing a robust colorimetric biosensor. Nanoscale, 2020, 12, 19420-19428.	2.8	52
33	Electrically Conductive Coordination Polymer for Highly Selective Chemiresistive Sensing of Volatile Amines. Inorganic Chemistry, 2018, 57, 541-544.	1.9	51
34	A pulse-driven sensor based on ordered mesoporous Ag2O/SnO2 with improved H2S-sensing performance. Sensors and Actuators B: Chemical, 2016, 228, 529-538.	4.0	48
35	Solvothermal synthesis of porous CuFe2O4 nanospheres for high performance acetone sensor. Sensors and Actuators B: Chemical, 2018, 270, 538-544.	4.0	45
36	Highly sensitive and selective detection of biothiols using graphene oxide-based "molecular beacon―like fluorescent probe. Analytica Chimica Acta, 2012, 731, 68-74.	2.6	44

#	Article	IF	CITATIONS
37	Vitamin C-assisted synthesis and gas sensing properties of coaxial In2O3 nanorod bundles. Sensors and Actuators B: Chemical, 2015, 220, 68-74.	4.0	44
38	Mesoporous ZnFe2O4 prepared through hard template and its acetone sensing properties. Materials Letters, 2016, 183, 378-381.	1.3	44
39	Highly sensitive and humidity-independent ethanol sensors based on In ₂ O ₃ nanoflower/SnO ₂ nanoparticle composites. RSC Advances, 2015, 5, 52252-52258.	1.7	42
40	Metal–organic frameworks derived tin-doped cobalt oxide yolk-shell nanostructures and their gas sensing properties. Journal of Colloid and Interface Science, 2018, 528, 53-62.	5.0	42
41	YSZ-based NO2 sensor utilizing hierarchical In2O3 electrode. Sensors and Actuators B: Chemical, 2016, 222, 698-706.	4.0	40
42	Template-free synthesis of novel In2O3 nanostructures and their application to gas sensors. Sensors and Actuators B: Chemical, 2013, 185, 32-38.	4.0	39
43	Highly enhanced NO2 sensing performances of Cu-doped In2O3 hierarchical flowers. Sensors and Actuators B: Chemical, 2015, 221, 297-304.	4.0	38
44	A low temperature operating gas sensor with high response to NO ₂ based on ordered mesoporous Ni-doped In ₂ O ₃ . New Journal of Chemistry, 2016, 40, 2376-2382.	1.4	38
45	Interface interaction of MoS2 nanosheets with DNA based aptameric biosensor for carbohydrate antigen 15–3 detection. Microchemical Journal, 2020, 155, 104675.	2.3	38
46	Gas sensor based on samarium oxide loaded mulberry-shaped tin oxide for highly selective and sub ppm-level acetone detection. Journal of Colloid and Interface Science, 2018, 531, 74-82.	5.0	35
47	Fluorescent hydrogel test kit coordination with smartphone: Robust performance for on-site dimethoate analysis. Biosensors and Bioelectronics, 2019, 145, 111706.	5.3	35
48	High-response and low-temperature nitrogen dioxide gas sensor based on gold-loaded mesoporous indium trioxide. Journal of Colloid and Interface Science, 2018, 524, 368-378.	5.0	34
49	Preparation of silver-loaded titanium dioxide hedgehog-like architecture composed of hundreds of nanorods and its fast response to xylene. Journal of Colloid and Interface Science, 2019, 536, 215-223.	5.0	33
50	Bifunctional Thiourea–Ammonium Salt Catalysts Derived from Cinchona Alkaloids: Cooperative Phase-Transfer Catalysts in the Enantioselective Aza-Henry Reaction of Ketimines. Journal of Organic Chemistry, 2018, 83, 1486-1492.	1.7	32
51	Hierarchical core/shell ZnO/NiO nanoheterojunctions synthesized by ultrasonic spray pyrolysis and their gas-sensing performance. CrystEngComm, 2016, 18, 8101-8107.	1.3	31
52	Facile synthesis of nitrogen and sulfur co-doped carbon dots for multiple sensing capacities: alkaline fluorescence enhancement effect, temperature sensing, and selective detection of Fe ³⁺ ions. New Journal of Chemistry, 2018, 42, 13147-13156.	1.4	26
53	Controlled synthesis of hierarchical Sn-doped α-Fe2O3 with novel sheaf-like architectures and their gas sensing properties. RSC Advances, 2013, 3, 7112.	1.7	23
54	STED Nanoscopy Imaging of Cellular Lipid Droplets Employing a Superior Organic Fluorescent Probe. Analytical Chemistry, 2021, 93, 14784-14791.	3.2	23

#	Article	IF	CITATIONS
55	Solvent-controlled synthesis of full-color carbon dots and its application as a fluorescent food-tasting sensor for specific recognition of jujube species. Sensors and Actuators B: Chemical, 2021, 342, 129963.	4.0	21
56	Detection of low concentration acetone utilizing semiconductor gas sensor. Journal of Materials Science: Materials in Electronics, 2020, 31, 5478-5484.	1.1	20
57	Monodisperse WO3 hierarchical spheres synthesized via a microwave assisted hydrothermal method: time dependent morphologies and gas sensing characterization. RSC Advances, 2014, 4, 23281.	1.7	17
58	Insight into the effect of the continuous testing and aging on the SO2 sensing characteristics of a YSZ (Yttria-stabilized Zirconia)-based sensor utilizing ZnGa2O4 and Pt electrodes. Journal of Hazardous Materials, 2020, 388, 121772.	6.5	17
59	Room-Temperature Mixed-Potential Type ppb-Level NO Sensors Based on K ₂ Fe ₄ O ₇ Electrolyte and Ni/Fe–MOF Sensing Electrodes. ACS Sensors, 2021, 6, 4435-4442.	4.0	16
60	Enhanced resistive acetone sensing by using hollow spherical composites prepared from MoO3 and In2O3. Mikrochimica Acta, 2019, 186, 359.	2.5	15
61	Amperometric H2S sensor based on a Pt-Ni alloy electrode and a proton conducting membrane. Sensors and Actuators B: Chemical, 2020, 311, 127900.	4.0	13
62	An enantioselective aza-Henry reaction of trifluoromethyl ketimines catalyzed by phase-transfer catalysts. Organic Chemistry Frontiers, 2019, 6, 3269-3273.	2.3	12
63	Asymmetric synthesis of spirooxindole–pyranoindole products <i>via</i> Friedel–Crafts alkylation/cyclization of the indole carbocyclic ring. New Journal of Chemistry, 2020, 44, 9788-9792.	1.4	12
64	Cadmium sulfide in-situ derived heterostructure hybrids with tunable component ratio for highly sensitive and selective detection of ppb-level H2S. Journal of Colloid and Interface Science, 2022, 627, 332-342.	5.0	8
65	Highly Selective Solidâ€Phase Extraction of Pb(II) by Ionâ€Imprinted Superparamagnetic Mesoporous Silica. ChemistrySelect, 2019, 4, 259-264.	0.7	7
66	Enantioselective addition of thiols to trifluoromethyl ketimines: synthesis of <i>N</i> , <i>S</i> -ketals. Organic and Biomolecular Chemistry, 2020, 18, 7431-7436.	1.5	6
67	Highly sensitive mixed-potential type ethanol sensors based on stabilized zirconia and ZnNb2O6sensing electrode. RSC Advances, 2016, 6, 27197-27204.	1.7	5
68	One-step synthesis and gas sensing properties of hierarchical SnO2 materials. Chemical Research in Chinese Universities, 2013, 29, 837-840.	1.3	4